Machine Learning-Assisted Array Synthesis Using Active Base Element Modeling

Qi Wu [1], Weiqi Chen [2], Chen Yu [2], Haiming Wang [2], and Wei Hong [2]

[1]Southeast University
[2]Affiliation not available

October 30, 2023

Abstract

Array synthesis under practical constraints is a vital design task. Traditional array synthesis methods usually deal with isolated antenna elements without considering mutual coupling (MC) or mounting-platform effects, which results in unacceptable degradation in practical array designs. An efficient machine learning-assisted array synthesis (MLAAS) method is introduced using efficient active base element modeling (ABEM). This method greatly extends the boundaries of practical antenna array synthesis from the perspectives of both accuracy and design freedom. Using much fewer samples than those in conventional MLAAS methods, all possible element designs are accurately modeled into one active base element (ABE). Compared with conventional active element pattern (AEP)-based methods, the ABEM aims to predict AEPs for elements with arbitrary allocations and electromagnetic (EM) surroundings, therefore offering more degrees of freedom for practical array designs. Four array design examples are used to verify the effectiveness of the proposed method.

Machine Learning-Assisted Array Synthesis Using Active Base Element Modeling

Qi Wu, *Member, IEEE*, Weiqi Chen, *Student Member, IEEE*, Chen Yu, *Member, IEEE*, Haiming Wang, *Member, IEEE*, and Wei Hong, *Fellow, IEEE*

***Abstract*—Array synthesis under practical constraints is a vital design task. Traditional array synthesis methods usually deal with isolated antenna elements without considering mutual coupling (MC) or mounting-platform effects, which results in unacceptable degradation in practical array designs. An efficient machine learning-assisted array synthesis (MLAAS) method is introduced using efficient active base element modeling (ABEM). This method greatly extends the boundaries of practical antenna array synthesis from the perspectives of both accuracy and design freedom. Using much fewer samples than those in conventional MLAAS methods, all possible element designs are accurately modeled into one active base element (ABE). Compared with conventional active element pattern (AEP)-based methods, the ABEM aims to predict AEPs for elements with arbitrary allocations and electromagnetic (EM) surroundings, therefore offering more degrees of freedom for practical array designs. Four array design examples are used to verify the effectiveness of the proposed method.**

***Index Terms*—Antennas, arrays, machine learning, mutual coupling, platform effects, active base element modeling**

I. INTRODUCTION

ANTENNA array synthesis is one of the most important but difficult tasks in model radar and communication systems. In recent years, along with the increasing performance requirements from a system perspective, such as the gain, side-lobe level (SLL), directivity, reflection coefficient, isolation, multifrequency and broadband radiation, and polarization, practical antenna array designs have faced increasing design constraints from aspects ranging from the structure and fabrication process to the performance limitations of other radiofrequency (RF) devices. These requirements, constraints and limitations constrict the design space of conventional array synthesis and design methods. Moreover, although the development of computational electromagnetism (CEM) enables the creation of accurate responses for many real-world electromagnetic (EM) problems under sufficient time conditions, computationally intensive calculations make direct optimization using full-wave EM solvers impossible in practical antenna design problems, not to mention in antenna array designs within commercial compact devices or under complex EM environments.

Manuscript received June 11, 2021; revised Sept. 18, 2021; accepted Oct. 5, 2021. Date of publication ; date of current . This work was supported in part by the National Key R&D Program of China under Grant 2018YFB1801101, the National Natural Science Foundation of China under Grants 62001101 and 61960206006, the Science Foundation of Jiangsu Province of China under Grant BK20200349, the State Key Laboratory of Mobile Network and Mobile Multimedia Technology, ZTE Corporation, China, and the Fundamental Research Funds for the Central Universities.

The authors are with the State Key Laboratory of Millimeter Waves, Southeast University, Nanjing 210096, China, and with the Department of New Communications, Purple Mountain Laboratories, Nanjing 211111, China (e-mail: qiwu@seu.edu.cn; wq_chen@seu.edu.cn; chenyu@seu.edu.cn; hmwang@seu.edu.cn; weihong@seu.edu.cn). *(Corresponding author: Qi Wu, Haiming Wang.)*

Color versions of one or more of the figures in this paper are available online at http://ieeexplore.ieee.org.

Digital Object Identifier

A great number of excellent methods for finding optimized antenna arrays with proper element allocations and excitations have been proposed. These methods mainly include analytical methods [1], [2], stochastic optimization methods [3]–[5], compressive sensing (CS) [6] and many other hybrid methods, in which a majority of methods deal with isotropic elements, elements with patterns with simple analytical expressions or simulated isolated element patterns without consideration of mutual coupling (MC) or platform effects. While many of these methods are able to achieve great performance in acceptable time periods, these methods inevitably lead to beam quality degradation for practical design tasks due to MC and platform effects. On the other hand, the direct combination of CEM methods and optimization algorithms offers accurate but time-consuming choices for practical array design problems. The performance and computational complexity in modern antenna array design naturally contradict; this issue has drawn much attention in the last ten years.

Fortunately, this contradiction can be greatly ameliorated by introducing active element pattern (AEP)-based strategies into practical array design tasks [7]–[12]. In [10], the fast pattern synthesis of linear arrays is achieved using an iterative fast Fourier transform (FFT), in which the algorithm is expanded to unequally spaced linear array areas from equally spaced cases in [11] by introducing an excellent virtual AEP expansion method. While the proposed AEP-based strategies are able to deal with uniform or nonuniform arrays with great efficiency, most of them still focus on array designs with fixed element positions. In [9], an insightful iterative optimization approach based on AEPs and convex optimization for designing a circular array of horn antennas is proposed, in which the AEPs of the succeeding array design are estimated by assuming a phase-shifted version of their nearest simulated AEPs in previous full-wave simulations. In conclusion, there is still a long way to go before designers can "freely" modulate both array excitations and geometries, which relies on fast and accurate responses for both the AEPs and S-parameters of antenna elements under an arbitrary EM environment and MC and platform effects.

Over the last decade, machine learning (ML) methods have been widely investigated and applied in antenna and array designs due to their excellent ability to learn from simulated data sets through training processes and then make good predictions regarding potential design points [13]. Many ML methods, including artificial neural networks (ANNs) [14], Gaussian process regression (GPR) [15], [16] and support vector machines [17], have been introduced to build surrogate models for antenna elements and then applied to ML-assisted optimization (MLAO) schemes for EM component designs. Many great works have been introduced to solve array design tasks [18]–[22] and achieve excellent performance. While many MLAO-based algorithms have been proposed to alleviate the computational burden [23] and achieve better antenna performance [13], many become inadequate when EM problems become very complex if only data-driven strategies are considered in the construction of surrogate models.

Therefore, in regard to practical antenna array design problems, most researchers tend to seek hybrid algorithms that combine variable fidelity ML-based data-driven strategies and physical-based methods to achieve efficient surrogate model construction for the whole array. In [20], models with variable fidelity have been introduced to optimize for both SLL and S_{11} for a practical antenna array, which show great reduction of computational burden. While the initial intention of introduction of the ML method is to model the whole array performance under MC [24], recent studies have switched to building surrogate models for AEPs and letting the conventional array synthesis method deal with the rest [25]–[27], which is apparently more practical considering the large computational costs for numbers of full-wave antenna array simulations. One great improvement of these MLAO-AEP-based algorithms is that they can easily deal with antenna arrays with free element positions; in other words, they offer another degree of freedom in antenna array design. In [26], an ANN is introduced to build very accurate surrogate models for AEPs under variable element location distributions, which greatly helps to optimize single beam, square-cosecant beam and flat top beam patterns of microstrip antenna arrays.

The computational burden becomes nonnegligible when dealing with antenna array design problems using MLAO-AEP-based algorithms. In [26] and [25], approximately 1000 full-wave simulation samples are required to build surrogate models with enough accuracy for arrays with element numbers of approximately 10. In [27], 286 samples are simulated for a 5 element antenna array design. Considering the computational burden of building the initial data sets for the learning process of ML methods, these MLAO-AEP-based methods may be less practical than they initially appear to be. Good performance and heavy computational complexity are still contradictory after many years of development in antenna array design methodologies.

In this work, an efficient ML-assisted array synthesis (MLAAS) method is introduced to achieve fast active base element modeling (ABEM). Compared with conventional MLAO-AEP-based algorithms, the proposed method needs much less data to build a virtual active element model with which the AEPs and S-parameters of any elements with arbitrary allocations and EM surroundings can be accurately predicted. The proposed method offers more degrees of design freedom for practical array design and is validated using several antenna array design examples. The modeling method is presented in Section II. With the application of the proposed ABEM-based MLAAS method, the efficient array design is proposed in Section III. Section V concludes the whole work.

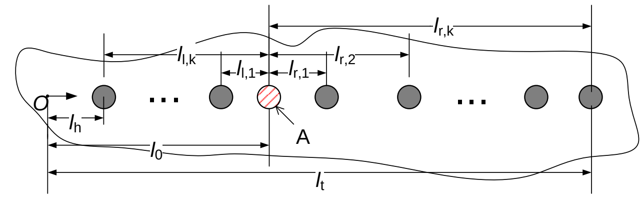

Fig. 1. Antenna element under MC and platform effects.

II. Machine Learning-Assisted Active Base Element Modeling

This section presents the ML-assisted ABEM method. Consider a linear antenna array with N elements located on the x-axis. As illustrated in Fig. 1, the characteristics of one antenna element can be fully defined using three items: the absolute element positions, relative element positions and array parameters. The absolute element position l_0 defines the absolute position of the concerned element. The relative element positions include $l_{l,1}, l_{l,2}, ..., l_{l,k}$ and $l_{r,1}, l_{r,2}, ..., l_{r,k}$, which define the relative distance between the concerned element and the elements on the left side and right side of the element, respectively. The subscript $1, 2, ..., k$ indicates the index of the adjacent elements. The two design parameters l_h and l_t are introduced to represent the allocations of the entire array at the platform, representing the coordinates of the head element and the trailer element, respectively. The far-field radiation pattern of the proposed array fed by a complex excitation ω_n, with $n = 1, ..., N$, can be written as

$$F(\theta) = \sum_{n=1}^{N} E_n(\theta)\omega_n e^{jux_n} \tag{1}$$

where $u = 2\pi \cos\theta$, E_n represents the AEP of the element n and x_n is the location of element n in wavelength.

As shown in Fig. 2, conventional MLAO-AEP-based design methods view the antenna array as an integrated EM structure, based on which the entire location distributions are seen as the input information, and the AEPs and active S-parameters of the fixed elements are seen as the characteristics under the given distribution and EM environment. These array distribution modeling (ADM) methods have two main limitations. First, the prediction ability of the learned surrogate models is limited due to the fixed numbers of antenna elements. In other words, the learned model can predict only the characteristics of a potential antenna array with element numbers the same as the training data. Second, the correlations between elements with different locations are ignored, which strongly limits the performance of the learned models, especially under a limited number of full-wave simulations.

Instead of considering the entire structure of the array as the input vectors, here, by considering every element as an

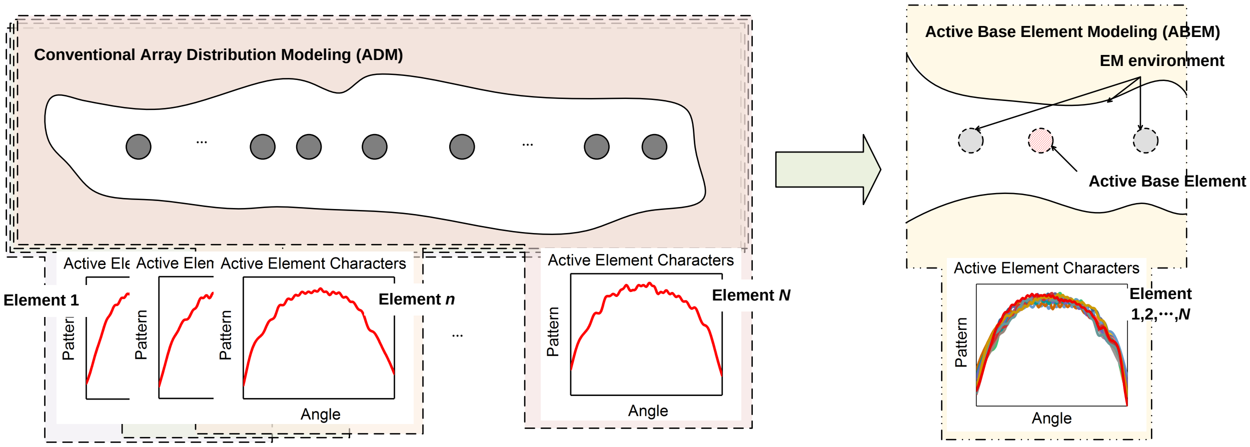

Fig. 2. Comparison between the proposed ABEM and conventional ADM.

identical active base element (ABE) with different allocations and EM surroundings, the ABE model is established with input vectors including the relative and absolute positions of the element and variable platform parameters and output characters including both magnitude and phase AEPs and active S-parameters. The absolute element positions $\mathbf{x}_\mathrm{a}$ and platform parameters $\mathbf{x}_\mathrm{p}$ are fetched directly, and all possible elements share similar data structures with these two characters. The relative positions of the element are defined using the following equation:

$$\mathbf{x}_{\mathrm{r},k} = \begin{cases} 1/\mathbf{l}_{\mathrm{r},k}, & \text{if the adjacent } k\text{-th element exists,} \\ 0, & \text{otherwise,} \end{cases} \tag{2}$$

in which $\mathbf{l}_{d,k}$ represents the relative distance between the modeled element and the adjacent k-th element, with $k = 1, 2, 3, ..., K$. For a linear array, both the left and right adjacent elements should be considered. On the one hand, the relative positions defined using Equation (2) are able to portray the MC effects of the adjacent elements with the reciprocal of their distances from the concerned element, and the condition of no adjacent elements is equally viewed as elements an infinite distance away. On the other hand, by controlling K, the number of adjacent elements taken into consideration can be easily manipulated to achieve a balance between the computational burden and prediction ability of the modeling process. Therefore, an M-element set of training data (i.e., simulated using a full-wave simulator with a finely discretized mesh) can be expressed as

$$\mathbf{D} = \{(\mathbf{u}_m, \mathbf{y}_m) | m = 1, 2, ..., M\} \tag{3}$$

with P-dimensional input vectors

$$\mathbf{u}_m = [\mathbf{x}_{\mathrm{a},m}\ \mathbf{x}_{\mathrm{p},m}\ \mathbf{x}_{\mathrm{r},m,1}\ \mathbf{x}_{\mathrm{r},m,2}\ ...\ \mathbf{x}_{\mathrm{r},m,K}\ f_m\ \theta_m]^T \tag{4}$$

and target output vectors

$$\mathbf{y}_m = [E_{\mathrm{mag},m}\ E_{\mathrm{pha},m}\ S_m]^T \tag{5}$$

in which f_m and θ_m represent frequency and angle values within the range of interest. Hence, $P = N_\mathrm{a} + N_\mathrm{p} + 2K + 2$, where N_a and N_p represent the dimensions of the absolute element positions and platform parameters.

For practical linear antenna array design tasks, the radiation pattern in the upper half plane at several frequency points of interest is often considered. The collected element numbers of the training data set can be expressed as $M = NM_\mathrm{fre}M_\mathrm{ang}M_\mathrm{sam}$, where M_fre, M_ang and M_sam are the numbers of concerned frequency points, angle points and sampled array location distributions. Hence, the dimensions of the overall data set are $M \times P$.

In antenna array conditions in which the size of the training sets produced by full-wave EM simulations is strictly limited, possible overfitting when applying an ANN is inevitable. The ML method GPR has recently received extensive attention in the field of EM, especially for antenna element optimization and design, due to its improved generalization capability compared with that of ANNs. In GPR, whereas a probability distribution describes random variables that are scalars or vectors, a stochastic process governs the properties of functions [28]. Here, three single output-GPR models are introduced to approximate the target output $y = f(\mathbf{x})$ of the magnitude and phase AEPs and S-parameters. The outputs are all interpreted as a probability distribution in function space as

$$f \sim \mathcal{GP}\left(m(\mathbf{u}), k(\mathbf{u}, \mathbf{u}')\right), \tag{6}$$

where $\mathbf{u}$ and $\mathbf{u}'$ are the positions in the $\mathbb{R}^P$ design space, $m(\mathbf{u})$ is the mean and $k(\mathbf{u}, \mathbf{u}')$ is the covariance function. Considering that the different types of input parameters have different effects on the output characteristics, covariance functions with separate length scales for each predictor are implemented and optimized for the final GPR models. One classic covariance function squared exponential (SE) kernel can be expressed as

$$k_\mathrm{SE}(\mathbf{u}, \mathbf{u}') = \sigma_\mathrm{f}^2 \exp\left(-\frac{1}{2}\sum_{p=1}^{P}(\mathbf{u} - \mathbf{u}')^2/\sigma_\mathrm{p}^2\right), \tag{7}$$

where σ_p represents the length scale of the p-th predictor, $p = 1, 2, ..., P$, which can be utilized to describe the correlations between two candidate designs, and σ_f is the output

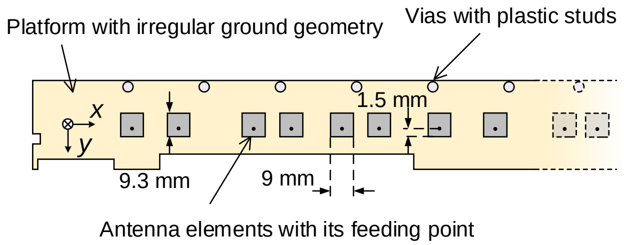

Fig. 3. Microstrip antenna array with N elements.

TABLE I
RMSEs OF MICROSTRIP ANTENNA ARRAYS WITH DIFFERENT K VALUES.

K	0	1	2	3	4
AEP (Mag.)	1.0690	0.2592	0.2413	0.2418	0.2494
AEP (Pha.)	0.1222	0.0409	0.0418	0.0405	0.0397
S-para.	0.2450	0.1040	0.1022	0.0828	0.0828

scale amplitude. The abovementioned hyperparameters are then determined in the training stage.

Consider a practical microstrip antenna array under complex EM surroundings and the irregular platform illustrated in Fig. 3. The concerned antenna element operates at 10 GHz with element numbers N ranging from 6 to 16. The modulation range for the element distribution is limited to within $0.4\lambda - \lambda$ for the adjacent elements. The antenna array is designed based on a platform with irregular ground and substrate geometry and multiple vias with plastic studs. The AEPs of the antenna element are severely affected by MC and platform effects, therefore leading to difficulties in the array design. Based on this practical prototype, the proposed ABEM method is investigated.

A. Effect of K

The parameter K defines the numbers of adjacent elements in the learned ABE model, which represents the MC effects of the K-nearest elements. The training sets and validation sets are established using high-fidelity full-wave simulation with $M_{\text{sample}} = 5$ for each $N = 6, 7, ..., 16$. The training data are selected from the original data set at a proportion of $r_{\text{t}} = 80\%$, with validation sets of $r_{\text{v}} = 20\%$. Note that both training and validation data sets are randomly selected within arbitrary numbers of N. The GPR models for the AEPs and S-parameters are learned with an optimization process for kernel functions and then hyperparameters. The Matern $5/2$ kernel function with different length scales for each predictor is selected after the optimization process.

The root mean square error (RMSE) is introduced to measure the prediction capability of the surrogate models produced using different K and is shown in Table I, with 2 typical validation cases shown in Fig. 4. Two important observations can be made. First, surrogate models with $K = 0$, which means that only isolated elements are considered, are not able to predict the character of AEPs under an array environment. Second, while the increase in K from 0 to 1 significantly improves the prediction capability of the surrogate models, the improvement is not notable when K is further increased. The selection of K relies on the EM character of the designed array, which in this case should be 1 to achieve a balance between prediction ability and computational burden.

TABLE II
RMSEs OF MICROSTRIP ANTENNA ARRAYS WITH DIFFERENT r_s VALUES.

r_s	0.500	0.200	0.100	0.050
AEP (Mag.)	0.3590	0.3224	0.3275	0.2320
AEP (Pha.)	0.0444	0.0439	0.0438	0.0317
r_s	0.020	0.010	0.005	0.002
AEP (Mag.)	0.3355	0.4381	0.5117	0.5621
AEP (Pha.)	0.0444	0.0683	0.0818	0.1020

B. Effect of the Sampling Ratio

While conventional MLAO-AEP-based algorithms require hundreds or thousands of allocation distribution vectors to achieve good prediction capabilities, the proposed ABE-based modeling methods can make good predictions based on limited data size. Similar to other data-driven surrogate model-based optimization methods for antenna design, the prediction ability and the computational burden naturally contradict during the modeling and optimization process. Moreover, unlike the cases in antenna element designs, in which the radiation performance at certain directions, such as broadside, are most concerned, the surrogate models in array synthesis problems need to cover much more beam directions to fully model the AEPs. For practical antenna array design algorithms, a large part of the computational burden comes from the learning process, which heavily relies on the data size. Therefore, for an efficient modeling process using GPR, the size of the data set is diluted using sampling ratio r_s.

Investigations on the effect of the sampling ratio are implemented using a practical microstrip array, with concerned angle points $M_{\text{ang}} = 181$. With $N = 15$, $M_{\text{sample}} = 5$, r_{t} = 0.8, and r_{v} = 0.2, random selection is implemented on the data set for sampling ratios r_s = 0.2, 0.1, 0.05 and 0.025 for both magnitude and phase patterns. As shown in Table II, as the sampling ratio decreases, the prediction ability of the surrogate model deteriorates moderately, which means that fewer data can be introduced in the training process without losing many capabilities to capture the character of the AEPs. It is worth mentioning that, in the optimization method MLAAS stated below, the sampling rate r_s for the initial data set is smaller compared with r_s for additional data set in every iteration, which reflects their difference in importance for the optimization process.

C. Prediction Capabilities Based on Training Sets with Different Element Numbers

One great advantage of the ABE-based modeling method is its capability of predicting AEPs for arbitrary array sizes, even based on training sets of different element numbers. To validate this merit, two different training data sets with the same data size are utilized to construct surrogate models for AEPs and are then introduced to predict AEPs under a certain

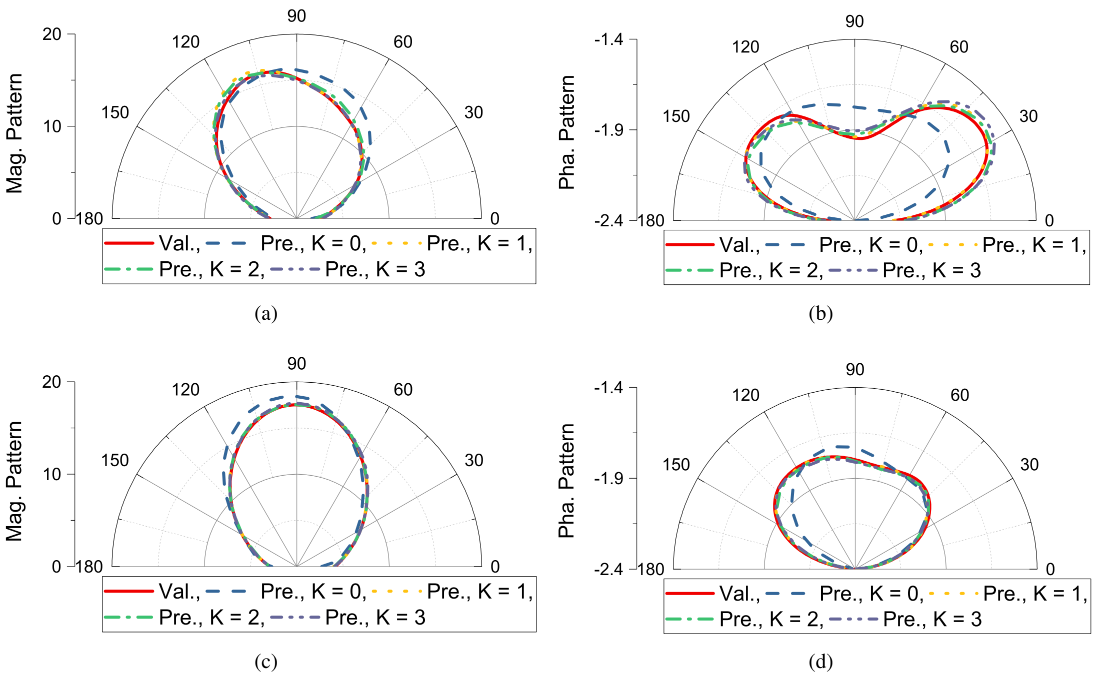

Fig. 4. Typical cases of predicted and validated AEPs with different K values.

TABLE III

RMSEs OF MICROSTRIP ANTENNA ARRAYS UNDER DIFFERENT CASES: CASE 1: NO SAMPLES WITH THE SAME ELEMENT NUMBER M_p AND CASE 2: HAVE SAMPLES WITH SAME ELEMENT NUMBER M_p..

ID	Case 1 (Mag.)	Case 2 (Mag.)	Case 1 (Pha.)	Case 2 (Pha.)
1	0.3842	0.4815	0.0624	0.0537
2	0.3833	0.3325	0.0633	0.0435
3	0.4305	0.2900	0.0712	0.0467
4	0.4035	0.3325	0.0657	0.0461
5	0.4462	0.3086	0.0693	0.0453

element number M_{p}. The first data sets include AEPs from arrays with element numbers $\mathbf{M}_{\mathrm{t1}}$ different from M_{p}, while the second data sets with $\mathbf{M}_{\mathrm{t2}}$ contain M_{p}. One typical result is shown in Table III with $M_{\mathrm{p}} = 8$, $\mathbf{M}_{\mathrm{t1}} = [6, 7, 9, 10]$ and $\mathbf{M}_{\mathrm{t2}} = [6, 7, 8, 9, 10]$. It is shown that with the introduction of the proposed ABEM, the constructed surrogate models are able to achieve high prediction accuracy even when based on training sets with different element numbers.

D. Comparison between ABEM and Array Distribution-Based Modeling

Conventional approaches always consider the entire array distribution as the input character for the established models. Compared with ADM, the proposed ABEM is not only able to deal with antenna arrays with arbitrary element numbers, as mentioned in the last subsection, but also able to achieve both greater prediction accuracy and a comparable computational burden. The microstrip antenna array shown in Fig. 1 with an element number of $N = 16$ is utilized to investigate the performance of the proposed ABEM. Both algorithms are utilized based on different training data set sizes, with the predicted AEPs validated. The calculated mean RMSEs for both magnitude and phase with data set sizes of 30 and 40 are shown in Fig. 5. The proposed ABEM shows obviously better performance than the conventional ADM, especially for a small number of samples. Moreover, with decreasing sample number, the ADM tends to fail to construct proper surrogate models within a limited number of optimizations due to its smaller input data sizes than ABEM. By viewing all elements as the base element with different input characteristics, the ABEM is able to utilize the information of the correlations between different antenna elements. Therefore, the ABEM is able to present a much better prediction ability than conventional ADM methods. With M = 30, the overall training times are 80.85 s and 80.85 s for the magnitude and phase pattern ADM, respectively, and are 86.57 s and 77.02 s when ABEM is used. With M = 40, the overall training times are 93.63 s and 93.63 s for magnitude and phase pattern ADM, respectively, and are 87.19 s and 95.16 s when ABEM is used. Therefore, with the application of the proposed ABEM, the surrogate models are able to achieve much higher prediction accuracy with a comparable computational burden.

III. Machine Learning-Assisted Array Synthesis

Based on the proposed ABEM method, an efficient MLAAS scheme for practical antenna array design is proposed in this section. The flow diagram of the MLAAS algorithm for array design is illustrated in Fig. 6. Detailed steps and technical considerations are given as follows.

Step 1. Initialization: In this step, the initial optimization and validation are first implemented based on the given prescribed design constraints, such as forbidden areas in the platform, and design goals, such as shaped radiation patterns, multibeam radiation patterns or S-parameters. Conventional optimization

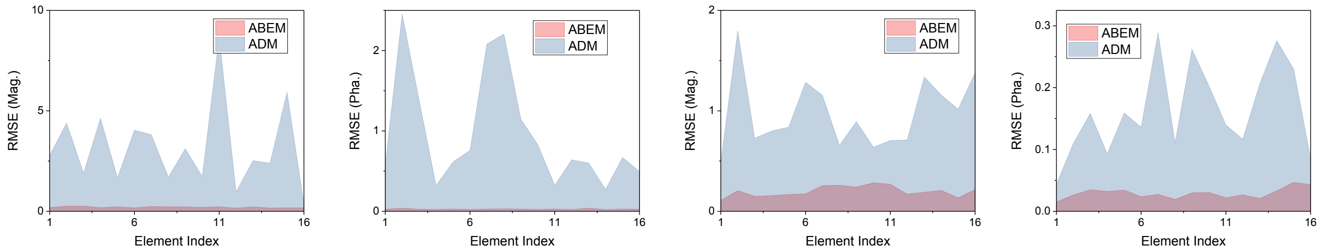

(a) (b) (c) (d)

Fig. 5. Prediction accuracy comparisons of ABEM and conventional ADM under different data set sizes. RMSEs of the (a) magnitude and (b) phase AEPs based on 30 samples and (c) magnitude and (d) phase AEPs based on 40 samples.

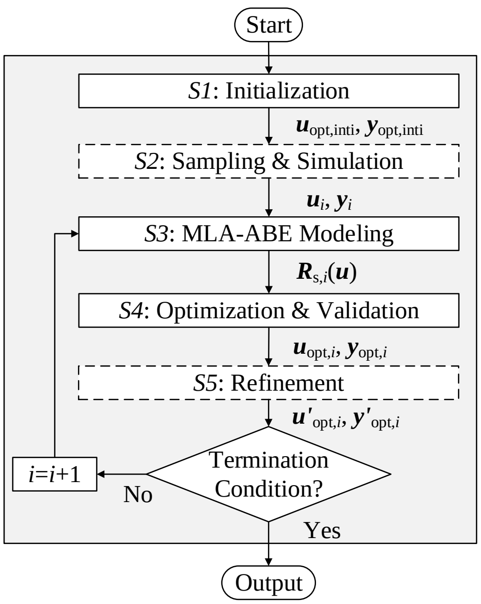

Fig. 6. Proposed algorithm for MLAAS.

methods based on ideal element radiation patterns are first implemented to allocate potential search areas in the design domain. The ideal element radiation pattern can be an omni-directional pattern, an analytical pattern, an isolated element pattern or a mean AEP calculated using previous design data. Then, the optimized array geometry and excitations $\boldsymbol{u}_{\text{opt, init}}$ are validated using full-wave EM simulation to find the actual AEPs, S-parameters and synthesized radiation patterns $\boldsymbol{y}_{\text{opt, init}}$. Normally, while the synthesized radiation pattern and S-parameters in this step cannot fulfill the predefined design goals due to the effects of the platform and MC effects, the acquired AEP and S data under this position distribution are potentially closely correlated to those in the final designs, which is therefore helpful in the modeling process.

Step 2. Sampling and Simulation: An optional step is introduced to enlarge the data set inherited from the first step. Different location distributions can be sampled based on random strategies, prior knowledge or uniform arrangements and then simulated using a full-wave EM simulator. The trade-off between the prediction accuracy and computational burden should be taken into consideration. Note that for many ML methods such as GPR, an increase in the size of the training set increases the computational burden of not only data preparation but also the prediction process. Considering the large number of predictions in the following optimization procedure, the selection of the training data is also important for efficient array design. The data set $\mathbf{D}_i = (\mathbf{u}_i, \mathbf{y}_i)$ is therefore established.

Step 3. MLA-ABE Modeling: In this step, surrogate models $\mathbf{R}_{\text{s},i}(\mathbf{u})$ for AEPs of magnitude and phase and S-parameters are constructed based on the above acquired training sets using ML methods. Here, GPR is utilized with the optimization process for suitable kernel functions and hyperparameters described in Section II.

Step 4. Optimization and Validation: Using the trained surrogate models, the optimization procedure is again implemented under the given restrictions and for predefined goals. For synthesis problems that can be transferred into convex optimization problems, iterative-convex optimization methods can be easily integrated into MLAAS. For those that can be solved only using evolutionary algorithms (EAs), all kinds of EAs can be introduced, in which the fitness functions are calculated based on the predictions of the trained surrogate models. Validation using a full-wave EM simulator is then applied, with data set $\mathbf{D}_{\text{opt},i} = (\mathbf{u}_{\text{opt},i}, \mathbf{y}_{\text{opt},i})$ established.

Step 5. Refinement: This optional step is introduced to alleviate the computational burden for EAs. In this step, the pattern performance is optimized based on a fixed element distribution that represents the validated AEPs and S-parameters obtained in Step 4. The results after refinement $\mathbf{D}'_{\text{opt},i} = (\mathbf{u}'_{\text{opt},i}, \mathbf{y}'_{\text{opt},i})$ are likely better than the optimized results obtained in Step 4 because the termination conditions in practical cases such as time or iterations are limited.

Step 6. Check if Terminated: In this step, the validated synthesized radiation pattern and S-parameters are checked to see if the termination condition has been fulfilled. If not, the validated data are added to the data set, and the algorithm returns to Step 3, where MLA-ABE modeling is again implemented with $i = i + 1$.

The proposed MLAAS follows the basic scheme of the MLAO proposed in [23], with a modeling procedure implemented using the proposed MLA-ABEM. Moreover, optional steps including Step 2 and Step 5 are added for better efficiency performance.

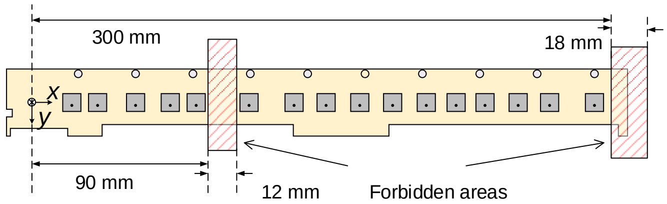

Fig. 7. Array geometry under forbidden platform area constraints in Case A.

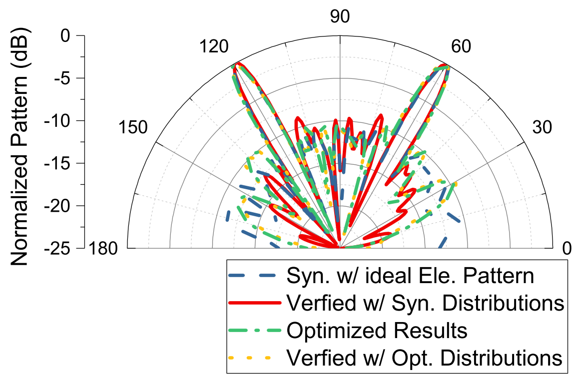

(a)

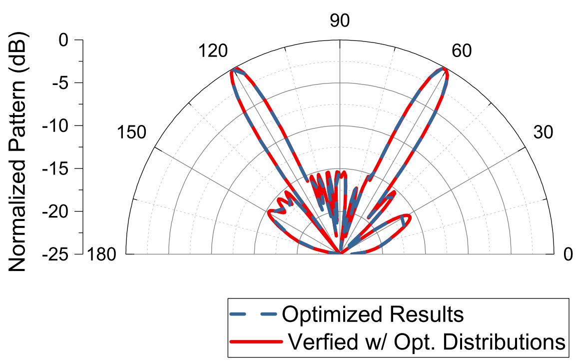

(b)

Fig. 8. Synthesized patterns from the proposed method at the initial step and the following 4 iterations in Case A. (a) Results at the initial step and the first step. (b) Results at the fourth step.

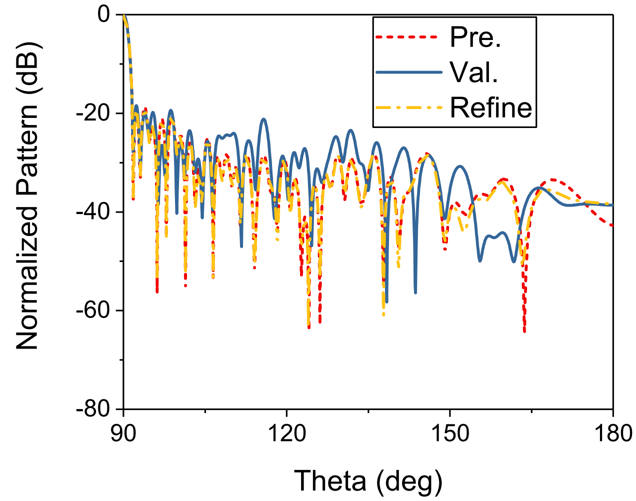

(a)

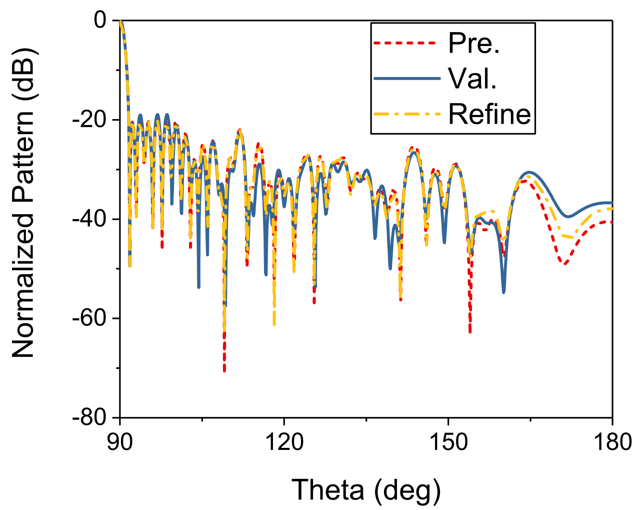

(b)

Fig. 9. Synthesized patterns from the proposed method at 2 iterations in Case B. (a) Results at first step. (b) Results at second step.

IV. Verification Examples

In this section, two different antenna array designs, including a microstrip antenna array with an irregular defective platform and a dielectric resonator antenna (DRA) array with metallic surroundings, are investigated and designed under various radiation requirements and restrictions. It is proven that the proposed MLAAS method is able to offer great design freedom, array performance and design efficiency and cooperate with various optimization methods.

A. Dual-Beam Pattern Synthesis with Platform Forbidden Area

First, a dual-beam pattern synthesis design task with forbidden areas on the platform is addressed using the proposed MLAAS algorithm based on the abovementioned microstrip antenna array. The element number is $N = 16$, and the designated beam directions are $\theta_1 = 60°$ and $\theta_2 = 120°$, with a 3-dB beamwidth smaller than 2°, and the SLL regions are defined as directions 7° away from beam directions. The platform is defective, with irregular forms, and is planted with multiple plastic screws. Two forbidden areas are defined to prevent the implementation of antenna elements. The gain differences between the two main beams are constrained within 0.2 dB. With the introduction of the proposed MLAAS combined with GA optimization, only a few iterations are needed to achieve great array performance. The model parameters are $N_\mathrm{a} = 1$, $N_\mathrm{p} = 2$, $K = 1$, $M_\mathrm{fre} = 1$, $M_\mathrm{ang} = 181$, and the overall data sizes in the final iteration are 28960×6 and 12452×6, which are sizes before and after sampling, respectively.

The optimized patterns are shown in Fig. 8, with the optimized array geometry illustrated in Fig. 7. As seen in Fig. 8(a), the verified results based on synthesized element distributions using ideal element patterns are deteriorated compared with the synthesized results due to MC and platform effects. The optimized results obtained in the first step based on the ABE models yield better pattern results than the

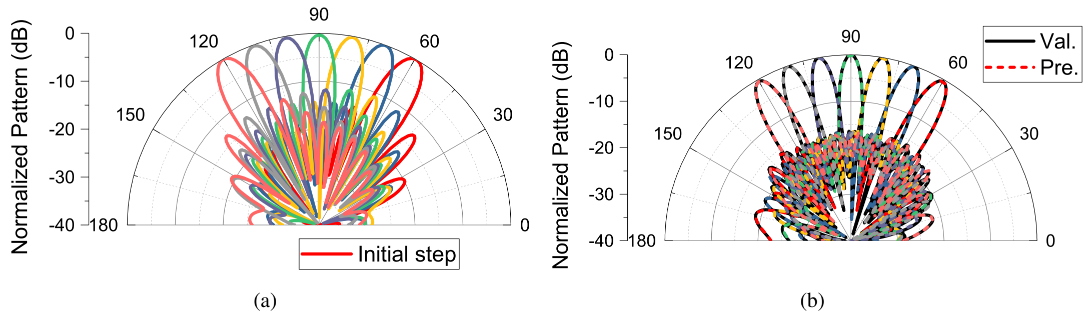

Fig. 10. Optimized patterns from the proposed method at the initial step and the final step in Case C: multibeam patterns at (a) the initial step and (b) the final step; typical AEPs at the final step: (c) phase patterns and (d) magnitude patterns.

verified results using synthesized distributions and provide good predictions compared with the verified results using the optimized distributions. In the following 3 iterations, combined with magnitude and phase refinement and the update of the ABE model, both great prediction accuracy and array pattern performance are achieved.

B. Minimum Element Number Optimization Under SLL Restriction

One of the greatest improvements of the proposed ABE-based modeling method is that designers are able to deal with optimization tasks with arbitrary element numbers. One practical example is the determination of the minimum element numbers under array performance restrictions, such as SLL restrictions, as shown in this subsection. Similar array platforms and element structures are utilized. The SLL restrictions are set as -20 dB, with the main direction angle $\theta_m = 90^\circ$, 3-dB beamwidth smaller than 0.3°, and SLL regions defined as directions 1.6° away from the beam direction. The model parameters are $N_\text{a} = 1$, $N_\text{p} = 2$, $K = 1$, $M_\text{fre} = 1$, $M_\text{ang} = 1801$, and the overall data sizes in the final iteration are 324180×6 and 5744×6, which are sizes before and after sampling, respectively. With the introduction of the proposed MLAAS, as shown in Fig. 9, with the initial element number of 50, desirable pattern performance can be achieved with a minimum element number N of 46 in the first iteration, and 44 in the second iteration. The RMSE of the array pattern is improved from 5.92 to 2.77 in the 2 calculated iterations.

C. Multibeam Optimization Using the Hybrid Convex-MLAO Method

The proposed MLAAS scheme is able to cooperate with arbitrary optimization methods. Recently, many great optimization methods for solving antenna array design problems have

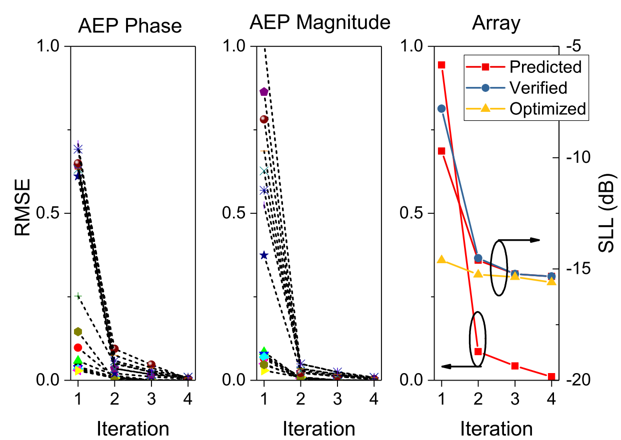

Fig. 11. RMSE of microstrip antenna element and array patterns during the optimization process in Case C.

been proposed, in which convex optimization has played an important role in achieving a more efficient design process than EAs. In [29], an insightful iterative approach using l_0-norm minimization is introduced to solve maximally sparse antenna array designs in the presence of MC. In [30], an excellent refined extended alternating convex optimization algorithm for solving multibeam sparse circular-arc antenna array designs is proposed. In [31], an iterative convex element position optimization algorithm for linear phased array synthesis with the aim of minimizing the SLL at multiple scan angles in the presence of MC is proposed. Here, as an example, the MLAAS scheme is combined with the methodology of the convex optimization algorithm to achieve multibeam optimization by predicting the AEPs using the proposed ABE modeling method.

Consider the design task with H different angles, in which ϕ_h represents the direction of maximum radiation for the

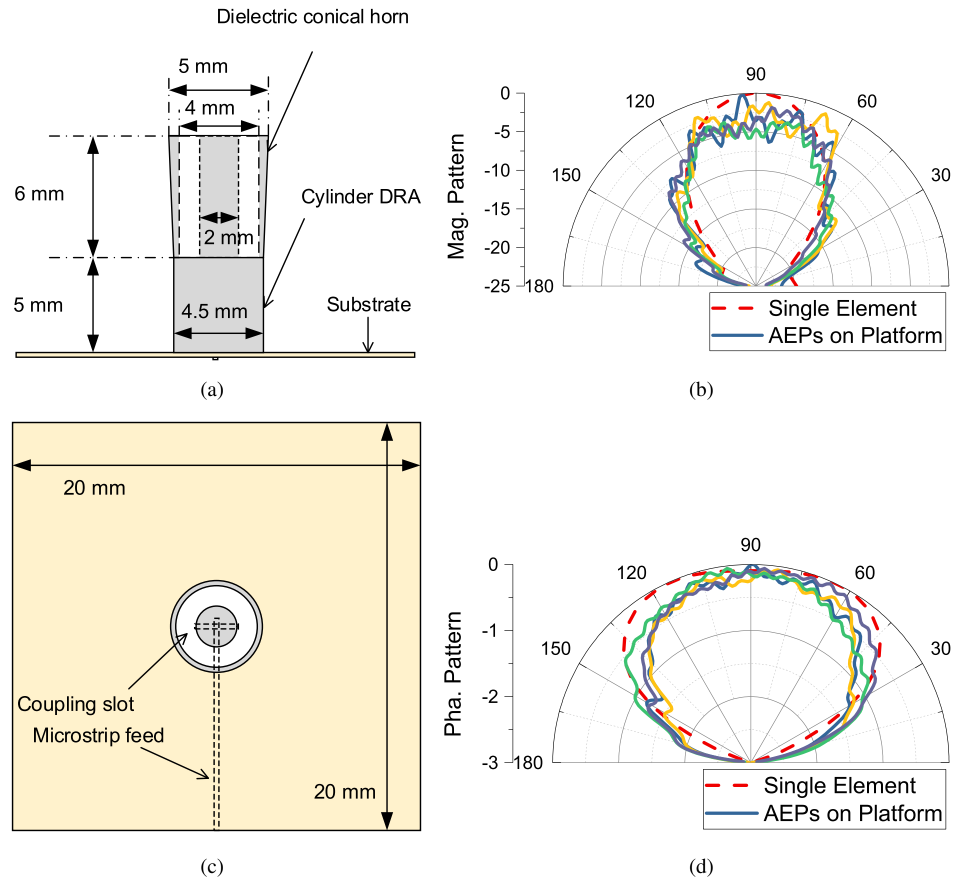

Fig. 12. DRA element geometry in Case D: (a) front view and (c) top view; element pattern of isolated elements and AEPs: (b) magnitude patterns and (d) phase patterns.

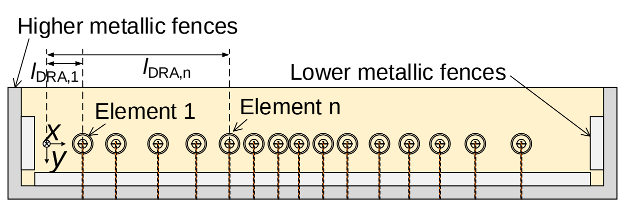

Fig. 13. Optimized DRA array geometry for flat-top pattern in Case D.

scanned beam with $h = 1, 2, ..., H$. Therefore, the weight of the n-th element for the scan angle ϕ_h is given by

$$\omega_{n,h} = e^{-jk_0\phi_h x_n}. \tag{8}$$

Considering a uniformly excited array, the predicted far-field radiation pattern is

$$\hat{F}^h(\theta) = \sum_{n=1}^{N} \hat{E}_n(\theta)\omega_n e^{j(u-u_h)x_n}. \tag{9}$$

where $u_h = 2\pi cos\theta_h$ and $\hat{E}_n$ is the predicted AEP based on the proposed AEB modeling method. Using the ideology of the first-order Taylor expansion, the far-field array pattern at the i^{th} iteration can be linearly approximated by

$$\hat{F}^{i,h}_{\epsilon_n}(\theta) \approx \sum_{n=1}^{N} \hat{E}^i_n(\theta)\omega_n e^{j(u-u_h)x_n^{i-1}}(1+j(u-u_h)\epsilon^i_n). \tag{10}$$

where x_n^{i-1} represents the element distribution at the previous iteration, and ϵ^i_n represents the position shift of the n^{th} element at the i^{th} iteration. Considering the design task of minimizing the SLL in the side lobe regions $\Theta_{SL,h}$ for each scan angle, the convex problem at the i^{th} iteration is defined as

$$\min_{\epsilon_i} \rho, s.t. \begin{cases} |\hat{F}^{i,h}_{\epsilon_i}(\Theta_{SL,h})| \leq \rho \text{ for } \forall h \\ |\epsilon_i| \leq \mu \\ D * (\epsilon_i + x^i) \geq d_{\text{min}} \end{cases} \tag{11}$$

where ρ is the maximum SLL limitation, μ is a predefined upper bound for the position shifts, and D is a circulant matrix for the minimum interelement spacing (d_{min}) limitation (see [32]). The convex optimization step is implemented within the MLAAS scheme during every iteration, with the optimized distributions validated using a full-wave simulator. The optimization parameters are set with element number $N = 16$, $d_{\text{min}} = 0.4\lambda$, initial interelement spacing $d_{\text{ini}} = 0.4\lambda$, $H = 7$, scanning angles $\phi_h = -30°, -20°, ..., 30°$, and $\mu = 0.02\lambda$. The model parameters are $N_{\text{a}} = 1$, $N_{\text{p}} = 2$, $K = 1$, $M_{\text{fre}} = 1$, $M_{\text{ang}} = 181$, $N = 16$, and the overall data sizes in the final iteration are 28960×6 and 5791×6, which are sizes before and after sampling, respectively. The patterns at the initial step and the final step are shown in Fig. 10 with multibeam patterns at (a) the initial step and (b) the final step and typical AEPs at the final step: (c) phase patterns and (d) magnitude patterns. And the RMSE of the element and array patterns during the

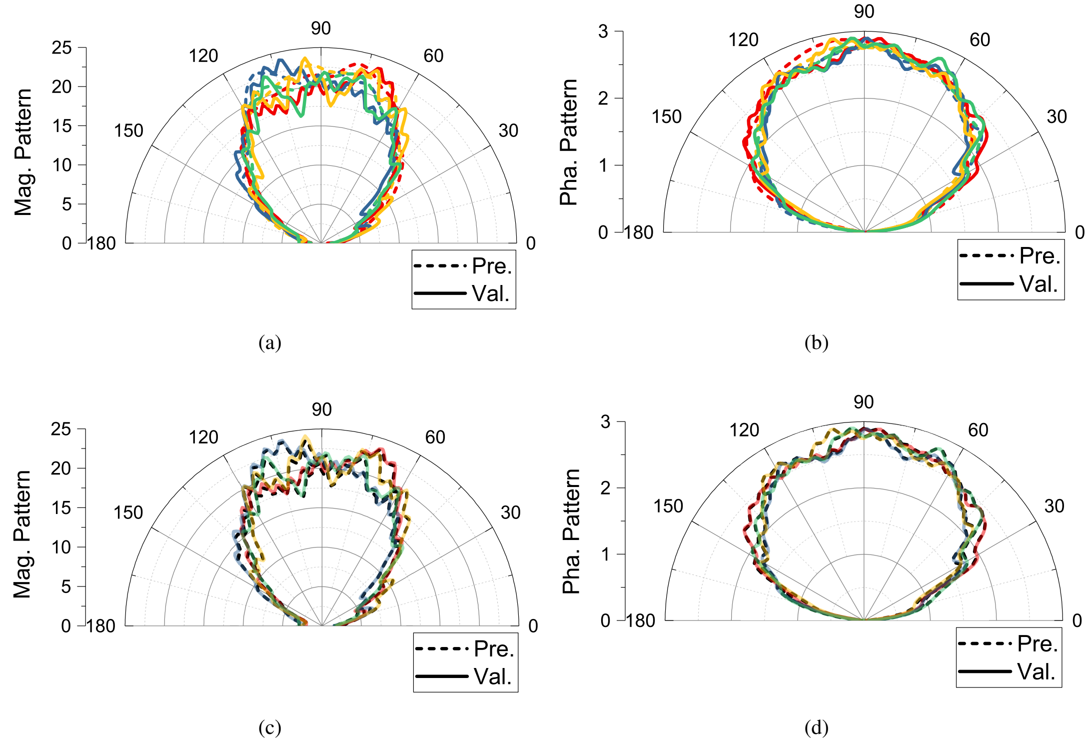

Fig. 14. Predicted and verified magnitude and phase AEPs in (a), (b) iteration 1 and (c), (d) iteration 2 in Case D.

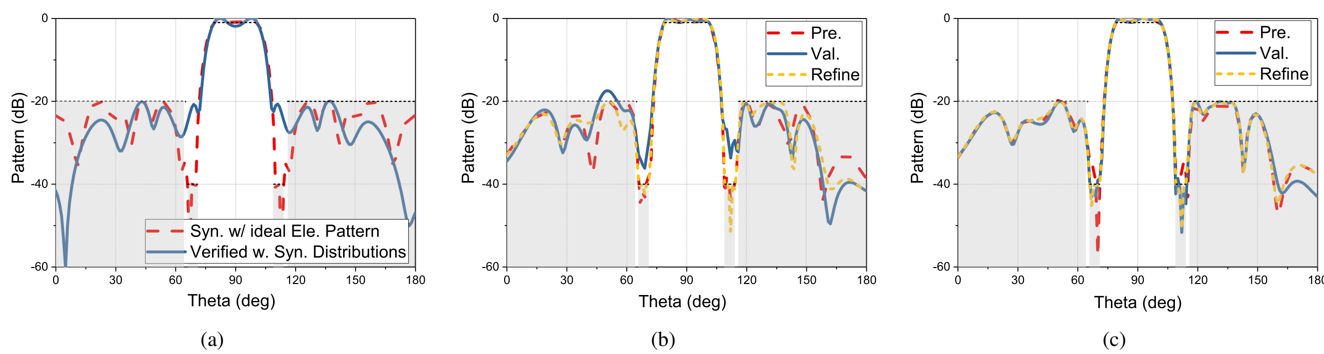

Fig. 15. Optimized patterns from the proposed method in Case D at (a) the initial step and (b)-(c) the following 2 steps.

optimization process is given in Fig. 11. The SLL is improved from -8.9 dB to -15.9 dB.

D. Flat-top Radiation Pattern Synthesis using a Dielectric Resonant Antenna Array

Another antenna array design is implemented based on the DRA element shown in Fig. 12 and Fig. 13 [33]. A cylindrical DRA (CDRA) built with $\epsilon_r = 5.7$ is excited using the microstrip line and the rectangular slot cut in the ground plane. Moreover, a truncated dielectric cone integrated on the top of the CDRA is added to improve the realized gain without reducing the overall antenna efficiency. As seen in Fig. 12, while the antenna element forms a smooth radiation pattern based on a ground plane with a limited size, the AEPs of the elements within an array with a large ground plane and metallic surroundings jitter intensely in the upper half-plane, which strongly affects the array performance.

The proposed MLAAS is utilized to synthesize a flat-top power pattern for a 16-element linear array based on the CDRA. Two kinds of metallic fences with different heights are placed around the elements. A similar pattern mask is utilized in [10] under fixed given element distributions. The MLAAS is able to deal with similar optimization tasks but with no predefined element distributions within only 2 iterations. The model parameters are $N_\mathrm{a} = 1$, $N_\mathrm{p} = 2$, $K = 1$, $M_\mathrm{fre} = 1$, $M_\mathrm{ang} = 181$, $N = 16$, and the overall data sizes in the final iteration are 23168×6 and 6660×6, which are sizes before and after sampling, respectively. The predicted and verified AEPs are shown in Fig. 14. As seen in Fig. 15 (a), the verified pattern obtained at the initial step is severely deteriorated compared with the synthesized pattern, failing to maintain good performance in both the main lobe and side lobe regions. As shown in Fig. 15 (b) and (c), with the increase in the prediction accuracy in the 2 iterations of the algorithm, the obtained pattern performance ultimately fulfills the predefined mask.

V. Conclusion

An MLAAS method has been proposed based on the efficient ABEM method. With the consideration of a limited range of surroundings and platform geometries, the ABE model can be established in a fast and accurate manner. The proposed ABEM has been investigated in detail and compared with conventional approaches. Based on the proposed modeling method, most array design tasks can be easily accomplished within a few iterations, which greatly accelerates the antenna array design process. Four practical design tasks, including pattern synthesis with a platform forbidden area, minimum element number optimization under SLL restrictions, multi-beam optimization using the hybrid convex-MLAO method and flat-top pattern synthesis with a DRA array, have been implemented to validate the effectiveness of the proposed method.

VI. Acknowledgment

The authors would like to thank the editors and the anonymous reviewers for their valuable comments and suggestions.

References

[1] O. M. Bucci, M. D'Urso, T. Isernia, P. Angeletti, and G. Toso, "Deterministic synthesis of uniform amplitude sparse arrays via new density taper techniques," *IEEE Trans. Antennas Propag.*, vol. 58, no. 6, pp. 1949–1958, 2010.

[2] Y. Liu, Q. H. Liu, and Z. Nie, "Reducing the number of elements in multiple-pattern linear arrays by the extended matrix pencil methods," *IEEE Trans. Antennas Propag.*, vol. 62, no. 2, pp. 652–660, 2013.

[3] S. K. Goudos, K. A. Gotsis, K. Siakavara, E. E. Vafiadis, and J. N. Sahalos, "A multi-objective approach to subarrayed linear antenna arrays design based on memetic differential evolution," *IEEE Trans. Antennas Propag.*, vol. 61, no. 6, pp. 3042–3052, 2013.

[4] M. M. Khodier and C. G. Christodoulou, "Linear array geometry synthesis with minimum sidelobe level and null control using particle swarm optimization," *IEEE Trans. Antennas Propag.*, vol. 53, no. 8, pp. 2674–2679, 2005.

[5] S.-H. Yang and J.-F. Kiang, "Optimization of sparse linear arrays using harmony search algorithms," *IEEE Trans. Antennas Propag.*, vol. 63, no. 11, pp. 4732–4738, 2015.

[6] G. Oliveri, M. Carlin, and A. Massa, "Complex-weight sparse linear array synthesis by bayesian compressive sampling," *IEEE Trans. Antennas Propag.*, vol. 60, no. 5, pp. 2309–2326, 2012.

[7] D. F. Kelley and W. L. Stutzman, "Array antenna pattern modeling methods that include mutual coupling effects," *IEEE Trans. Antennas Propag.*, vol. 41, no. 12, pp. 1625–1632, 1993.

[8] L. Caccavale, F. Soldovier, and T. Isernia, "Methods for optimal focusing of microstrip array antennas including mutual coupling," *IEE Proc.-Microw. Antennas Propag.*, vol. 147, no. 3, pp. 199–202, 2000.

[9] C. Bencivenni, M. Ivashina, R. Maaskant, and J. Wettergren, "Synthesis of maximally sparse arrays using compressive sensing and full-wave analysis for global earth coverage applications," *IEEE Trans. Antennas Propag.*, vol. 64, no. 11, pp. 4872–4877, 2016.

[10] Y. Liu, X. Huang, K. Da Xu, Z. Song, S. Yang, and Q. H. Liu, "Pattern synthesis of unequally spaced linear arrays including mutual coupling using iterative FFT via virtual active element pattern expansion," *IEEE Trans. Antennas Propag.*, vol. 65, no. 8, pp. 3950–3958, 2017.

[11] X. Huang, Y. Liu, P. You, M. Zhang, and Q. H. Liu, "Fast linear array synthesis including coupling effects utilizing iterative FFT via least-squares active element pattern expansion," *IEEE Antennas Wireless Propag. Lett.*, vol. 16, pp. 804–807, 2016.

[12] A. F. Morabito, A. Di Carlo, L. Di Donato, T. Isernia, and G. Sorbello, "Extending spectral factorization to array pattern synthesis including sparseness, mutual coupling, and mounting-platform effects," *IEEE Trans. Antennas Propag.*, vol. 67, no. 7, pp. 4548–4559, 2019.

[13] Q. Wu, W. Chen, H. Wang, and W. Hong, "Machine learning-assisted tolerance analysis and its application to antennas," in *2020 IEEE International Symposium on Antennas and Propagation (ISAP)*. IEEE, 2020, pp. 1853–1854.

[14] Y. Kim, S. Keely, J. Ghosh, and H. Ling, "Application of artificial neural networks to broadband antenna design based on a parametric frequency model," *IEEE Trans. Antennas Propag.*, vol. 55, no. 3, pp. 669–674, 2007.

[15] B. Liu, H. Aliakbarian, Z. Ma, G. A. Vandenbosch, G. Gielen, and P. Excell, "An efficient method for antenna design optimization based on evolutionary computation and machine learning techniques," *IEEE Trans. Antennas Propag.*, vol. 62, no. 1, pp. 7–18, 2014.

[16] S. Koziel and S. Ogurtsov, "Multi-objective design of antennas using variable-fidelity simulations and surrogate models," *IEEE Trans. Antennas Propag.*, vol. 61, no. 12, pp. 5931–5939, 2013.

[17] D. R. Prado, J. A. López-Fernández, M. Arrebola, and G. Goussetis, "Support vector regression to accelerate design and crosspolar optimization of shaped-beam reflectarray antennas for space applications," *IEEE Trans. Antennas Propag.*, vol. 67, no. 3, pp. 1659–1668, 2018.

[18] S. Koziel, S. Ogurtsov, W. Zieniutycz, and L. Sorokosz, "Expedited design of microstrip antenna subarrays using surrogate-based optimization," *IEEE Antennas and Wireless Propag. Lett.*, vol. 13, pp. 635–638, 2014.

[19] ——, "Simulation-driven design of microstrip antenna subarrays," *IEEE Trans. Antennas Propag.*, vol. 62, no. 7, pp. 3584–3591, 2014.

[20] S. Koziel and S. Ogurtsov, "Fast simulation-driven optimization of planar microstrip antenna arrays using surrogate superposition models," *International Journal of RF and Microwave Computer-Aided Engineering*, vol. 25, no. 5, pp. 371–381, 2015.

[21] R. Lovato and X. Gong, "Phased antenna array beamforming using convolutional neural networks," in *2019 IEEE International Symposium on Antennas and Propagation and USNC-URSI Radio Science Meeting*. IEEE, 2019, pp. 1247–1248.

[22] J. Tak, A. Kantemur, Y. Sharma, and H. Xin, "A 3-D-printed W-band slotted waveguide array antenna optimized using machine learning," *IEEE Antennas and Wireless Propag. Lett.*, vol. 17, no. 11, pp. 2008–2012, 2018.

[23] Q. Wu, H. Wang, and W. Hong, "Multistage collaborative machine learning and its application to antenna modeling and optimization," *IEEE Trans. Antennas Propag.*, vol. 68, no. 5, pp. 3397–3409, 2020.

[24] R. G. Ayestaran, F. Las-Heras, and L. F. Herrán, "Neural modeling of mutual coupling for antenna array synthesis," *IEEE Trans. Antennas Propag.*, vol. 55, no. 3, pp. 832–840, 2007.

[25] Y. Gong and S. Xiao, "Synthesis of sparse arrays in presence of coupling effects based on ANN and IWO," in *2019 IEEE international conference on computational electromagnetics (ICCEM)*. IEEE, 2019, pp. 1–3.

[26] Y. Gong, S. Xiao, and B.-Z. Wang, "An ANN-based synthesis method for nonuniform linear arrays including mutual coupling effects," *IEEE Access*, vol. 8, pp. 144 015–144 026, 2020.

[27] W. Chen, Z. Niu, and C. Gu, "Parametric modeling of unequally spaced linear array based on artificial neural network," in *2020 9th Asia-Pacific Conference on Antennas and Propagation (APCAP)*. IEEE, 2020, pp. 1–2.

[28] C. E. Rasmussen, "Gaussian processes in machine learning," in *Summer School on Machine Learning*. Springer, 2003, pp. 63–71.

[29] C. Bencivenni, M. Ivashina, R. Maaskant, and J. Wettergren, "Design of maximally sparse antenna arrays in the presence of mutual coupling," *IEEE Antennas Wireless Propag. Lett.*, vol. 14, pp. 159–162, 2014.

[30] Y. Liu, Y. Yang, P. Wu, X. Ma, M. Li, K.-D. Xu, and Y. J. Guo, "Synthesis of multibeam sparse circular-arc antenna arrays employing refined extended alternating convex optimization," *IEEE Trans. Antennas Propag.*, vol. 69, no. 1, pp. 566–571, 2020.

[31] Y. Aslan, M. Candotti, and A. Yarovoy, "Synthesis of multi-beam space-tapered linear arrays with side lobe level minimization in the presence of mutual coupling," in *2019 13th European Conference on Antennas and Propagation (EuCAP)*. IEEE, 2019, pp. 1–5.

[32] Y. Aslan, J. Puskely, A. Roederer, and A. Yarovoy, "Synthesis of multiple beam linear arrays with uniform amplitudes," in *12th European Conference on Antennas and Propagation (EuCAP 2018)*. IET, 2018, pp. 1–5.

[33] E. Baldazzi, A. Al-Rawi, R. Cicchetti, A. B. Smolders, O. Testa, C. d. J. van Coevorden Moreno, and D. Caratelli, "A high-gain dielectric resonator antenna with plastic-based conical horn for millimeter-wave

applications," *IEEE Antennas Wireless Propag. Lett.*, vol. 19, no. 6, pp. 949–953, 2020.

Qi Wu (S'15-M'19) was born in 1993. He received the B.S. degree in communication engineering from the Communication University of China, Beijing, China, in 2012, and M.S. and Ph.D. degrees in electrical engineering from Southeast University, Nanjing, China, in 2015 and 2019, respectively.

He joined the State Key Laboratory of Millimeter Waves, Southeast University, in March 2019. Now he is a Lecturer. From October 2016 to September 2017, he was a Junior Visiting Fellow at Ando and Hirokawa Laboratory, Tokyo Institute of Technology, Tokyo, Japan. His current research interest is AI-powered antenna and radiofrequency technologies (iART).

He has authored and co-authored over 40 technical publications in peer reviewed international journals and conference proceedings, and over 20 patents. He was the recipient of the Honorable Mention at the student contest of IEEE APS-URSI Conference 2018, selected as the Finalist in the IEEE EuCAP 2016, the student paper contest of iWAT 2018 and the best poster contest of iWAT 2019. He has served as a reviewer for the IEEE TRANSACTIONS ON ANTENNAS AND PROPAGATION, the IEEE ANTENNAS AND WIRELESS PROPAGATION LETTERS and the IEEE MICROWAVE AND WIRELESS COMPONENTS LETTERS.

Weiqi Chen (S'18) was born in 1995. She received the B.S. degree in electronic information science and technology from Nankai University, Tianjin, China, in 2018. She is currently pursuing the Ph.D. degree in electrical engineering from Southeast University, Nanjing, China. Her current research interest is AI-powered antenna and radiofrequency technologies (iART).

Chen Yu (M'11) was born in 1979. She received the M.S. and Ph.D. degrees in electrical engineering from Southeast University, Nanjing, China, in 2004 and 2011, respectively.

She joined the State Key Laboratory of Millimeter Waves, Southeast University, in April 2004. Now she is an Associate Professor. In 2007, she was a short-term Visiting Scholar at the Kalmar Institute of Technology, Sweden. Her current research interests include antennas and antenna arrays for wireless mobile communications and radars.

Dr. Yu received the first-class Science and Technology Progress Award of Jiangsu Province of China in 2009.

Haiming Wang (M'08) was born in 1975. He received the B.S., M.S., and Ph.D. degrees in Electrical Engineering from Southeast University, Nanjing, China, in 1999, 2002, and 2009, respectively.

He joined the School of Information Science and Engineering, Southeast University, Nanjing, China, in 2002, and is currently a distinguished professor. He is also a part-time professor with the Purple Mountain Laboratories, Nanjing, China. He has authored and co-authored over 50 technical publications in IEEE TRANSACTIONS ON ANTENNAS AND PROPAGATION and other peer-reviewed academic journals. Prof. Wang has authored and co-authored over more than 70 patents and 52 patents have been granted. He was awarded twice for contributing to the development of IEEE 802.11aj by the IEEE Standards Association in 2018 and 2020.

His current research interests include AI-powered antenna and radiofrequency technologies (iART), AI-powered channel measurement and modeling technologies (iCHAMM), and integrated communications and sensing (iCAS).

Wei Hong (M'92-SM'07-F'12) received the B.S. degree in radio engineering from the University of Information Engineering, Zhengzhou, China, in 1982, and the M.S. and Ph.D. degrees in radio engineering from Southeast University, Nanjing, China, in 1985 and 1988, respectively.

In 1993, he joined the University of California at Berkeley, Berkeley, CA, USA, as a Short-Term Visiting Scholar. From 1995 to 1998, he was a Short-Term Visiting Scholar with the University of California at Santa Cruz, Santa Cruz, CA, USA. Since 1988, he has been with the State Key Laboratory of Millimeter Waves, Southeast University, where he has been the Director since 2003. He is currently a Professor with the School of Information Science and Engineering, Southeast University. He has authored or co-authored over 300 technical publications and authored two books. His current research interests include numerical methods for electromagnetic problems, millimeter-wave theory and technology, antennas, electromagnetic scattering, and RF technology for mobile communications.

Dr. Hong was an Elected IEEE MTT-S AdCom Member from 2014 to 2016. He is a Fellow of Chinese Institute of Electronics (CIE). He was a recipient of the National Natural Prizes twice, the First-Class Science and Technology Progress Prizes thrice, issued by the Ministry of Education of China and Jiangsu Province Government, and the Foundations for China Distinguished Young Investigators and "Innovation Group" issued by the NSF of China. He is currently a Vice President of the CIE Microwave Society and Antenna Society and the Chair of the IEEE MTTS/APS/EMCS Joint Nanjing Chapter. He served as an Associate Editor for the IEEE TRANSACTIONS ON MICROWAVE THEORY AND TECHNIQUES from 2007 to 2010 and one of the guest editors for the 5G Special Issue of the IEEE TRANSACTIONS ON ANTENNAS AND PROPAGATION in 2017.